INVITED ARTICLE

Highly infrared transparent spark plasma sintered AlON ceramics

Yingchun Shan[a)]
Department of Materials Science and Engineering, Dalian Maritime University, Dalian 116026, China

Xialu Wei
College of Engineering, San Diego State University, San Diego, CA 92182, USA

Xiannian Sun and Jiujun Xu
Department of Materials Science and Engineering, Dalian Maritime University, Dalian 116026, China

Qinghua Qin
Research School of Engineering, Australian National University, Acton, ACT 2601, Australia

Eugene A. Olevsky[b)]
College of Engineering, San Diego State University, San Diego, CA 92182, USA

(Received 25 December 2016; accepted 3 March 2017)

Spark plasma sintering (SPS) is adopted to fabricate transparent AlON ceramics at 1350–1500 °C under 40 MPa, using a bimodal γ-AlON powder synthesized by the carbothermal reduction and nitridation method. After holding 10 min, high density samples are obtained, and their optical transmittance is investigated over the wavelength range of 1330–6000 nm. Despite the samples SPS-processed at 1350 °C indicate the presence of three-phases: γ-AlON, α-Al_2O_3, and h-AlN, they show high infrared transparency, i.e., the maximum transmittance for 1.2 mm thick specimens is up to 77.3% at ~3900 nm. Also, the processed samples exhibit high hardness of 17.81 GPa. The high infrared transmittance should be mainly attributed to high density and rationally controlled grain size distribution, and the high hardness is apparently caused by a small grain size.

I. INTRODUCTION

Spinel-structured aluminum oxynitride (γ-AlON) is an important single phase and stable solid solution ceramic within the Al_2O_3–AlN system.[1] Transparent AlON ceramics have attracted a growing interest as infrared/visible window material, transparent armor, and other extremely durable optics due to its high strength and high hardness, high resistance to rain and sand damage, and excellent optical transparency properties.[2–8] Transparent AlON can be fabricated by conventional pressureless sintering, hot pressing, or hot isostatic pressing.[2,9–12] However, conventional fabrication of AlON ceramics usually requires sintering of a green body at high temperature (≥1850 °C) for a long holding period (≥6 h).[13] Unfortunately, high sintering temperature and long holding time can easily lead to excessive grain growth and coarse microstructure, which, in turn, tend to decrease the hardness of the processed materials.[14]

Recently, our work has confirmed that AlON powder having a bimodal particle size distribution (PSD) can be more efficiently pressureless sintered under fast heating of 40 °C/min and a lower sintering temperature of 1820–1880 °C. More importantly, the holding time of pressureless sintering used to obtain transparent AlON utilizing this bimodal powder can be remarkably shortened down to 1.5–2.5 h.[15] It was revealed that the bimodal powder can keep its bimodal PSD throughout the whole sintering process and therefore it can be rapidly densified. At the early or middle stage of the pressureless sintering (before the formation of AlON, <1700 °C), the bimodal samples have an excellent gap filling and rearrangement ability. At the final stage of sintering, AlON grains in the bimodal samples can diffuse much faster due to the transient bimodal AlON grain size distribution inherited from the bimodal starting powder. Further investigation into the phase transformation and microstructure evolution of these pressureless sintered samples indicates that high heating rates enable the sintering mixtures to keep a near spherical shape bimodal PSD until phase transformation from Al_2O_3 to AlON is fully completed. Then mass transport between large to large, large to small, and small to small AlON grains can simultaneously happen at the final fast densification stage, which benefits the less active formation of pores and fast growth of AlON grains. Therefore, high heating rates play a key role for fast and better consolidation of the utilized bimodal AlON powder.

On the other hand, spark plasma sintering (SPS) has been recognized as one of the most attractive rapid

Contributing Editor: Eugene Medvedovski
Address all correspondence to these authors.
[a)]e-mail: shanychun@dlmu.edu.cn
[b)]e-mail: eolevsky@mail.sdsu.edu
DOI: 10.1557/jmr.2017.96

powder consolidation technologies. It provides heating rates up to hundreds of °C/min through the Joule heating effect which largely shortens the processing time. At the same time, the applied pressure during SPS also offsets the required processing temperature level. As a result, SPS allows the rapid compaction of highly dense ceramics at relatively lower temperatures and with shorter holding time compared to conventional powder processing techniques.[16–18] In addition, high heating rates of SPS are also helpful for obtaining high density and fine-grained products.[19,20] Therefore, SPS-processed specimens usually possess smaller grains compared to their conventionally sintered counterparts as the grain growth is both temperature and time dependent.

Temperature overshoot is a universal phenomenon for SPS, which is similar to a two-step sintering. Generally, two-step sintering is an efficient approach for obtaining fully dense small grain ceramics because it suppresses grain growth at the final stage of sintering.[21] Because of these unique features, SPS was selected in the present study to consolidate a bimodal AlON powder to obtain highly dense transparent ceramic components with small grains and excellent properties. Therefore, using bimodal AlON powder synthesized by the carbothermal reduction and nitridation (CRN) method as the starting material, the SPS process similar to the mentioned two-step method was developed to obtain small grain specimens with higher hardness. High density transparent AlON ceramics based on the three-phase system (AlON, α-Al_2O_3, and h-AlN) were prepared after holding during 10 min at 1350 °C by the SPS. At the same time, the obtained ceramics also demonstrated a high hardness.

II. EXPERIMENTAL

High purity nanosized γ-Al_2O_3 (DK410-2, Beijing DK Nanotechnology Co. LTD, China) and activated charcoal powder (Beilian Chemical Reagent Co., China) were used as the starting materials for the synthesis of AlON powder. In high purity nitrogen, single phase AlON powder was firstly synthesized by the CRN method inside a graphite furnace (a detailed fabrication process has been described in Ref. 15). After removing the possible carbon residues in the synthesized AlON powder at 640 °C for 4 h in air, 0.5 wt% Y_2O_3 (Grade C, Starck, Germany) was added into the obtained powder. Using Si_3N_4 grinding balls (having 5, 8, and 10 mm diameter and weight ratio at 1.7:1:1.3) as milling media, keeping the ball-to-powder weight ratio at 7:1, the mixture of powders of AlON and Y_2O_3 was processed in absolute ethyl alcohol at 170 rpm for 24 h into a bimodal powder. The detailed fabrication process of the bimodal AlON powder has been described in Refs. 15 and 22.

The phase composition of the synthesized AlON powder was characterized by X-ray diffractometry (XRD; D/Max-ULtima+, Rigaku, Tokyo, Japan) using Cu $K_{\alpha1}$ radiation as shown in Fig. 1. The PSD of the milled AlON powder was measured using laser particle size analyzer (Mastersizer 2000, Malvern Instruments, Malvern, United Kingdom), and its PSD is shown in Fig. 2. The morphology of the obtained mixture powders was observed by field-emission scanning electron microscopy (FESEM; supra 55, Zeiss, Jena, Germany) as shown in Fig. 3.

2.7 g of the obtained bimodal AlON powder were placed into a graphite die with a diameter of 15 mm and then sintered in a SPS apparatus (SPSS-515, Fuji Electronic Industrial Co., Ltd., Kawasaki, Japan) in vacuum. The sample was first heated to 1350 °C, 1400 °C, 1450 °C, and 1500 °C at a heating rate of 100 °C/min, respectively. Then, after holding for 10 min, the heating system was shut down and the furnace was cooled down to room temperature. The axial pressure was maintained at the level of 40 MPa during the entire sintering process. The sintered samples were subsequently ground and polished on both sides to a thickness of 1.2 mm for the following optical transmittance measurements.

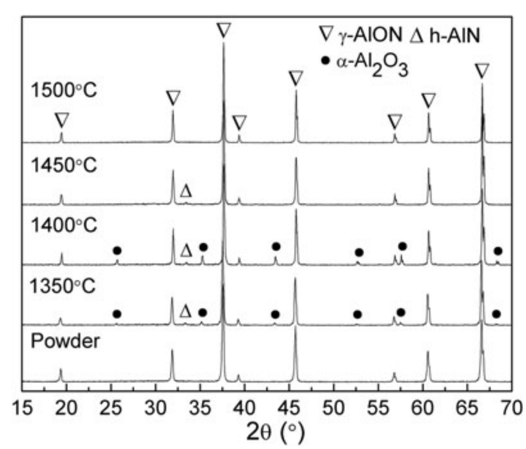

FIG. 1. XRD patterns of the AlON powder and the SPS-processed samples.

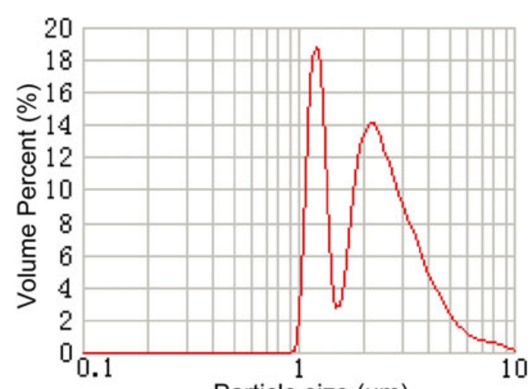

FIG. 2. Particle size distribution of the milled AlON powder.

The phase compositions of the sintered samples were characterized by XRD. The microstructure of sintered samples was observed using scanning electron microscope. The bulk density of the sintered samples was measured by the Archimedes method. Optical transmittance of all the fabricated samples in the wave range of 1330–6000 nm was recorded by a Fourier transform infrared spectroscopy (FTIR; Frontier, PE, USA). Vickers hardness at room temperature was measured by a hardness tester (M-400-H1, Leco Corp., St. Joseph, MI, USA) under a preset load of 1.0 kgf.

III. RESULTS AND DISCUSSION

A. Characteristics of AlON powder

The XRD pattern of the synthesized powder is shown in Fig. 1, which illustrates that single phase γ-AlON powder was synthesized by the CRN method and, as a result, only the γ-AlON crystalline phase was detected in the obtained powder. Figs. 2 and 3 present the PSD and the scanning electron microscopy (SEM) image of the milled powders, respectively. It can be observed that the synthesized single phase γ-AlON powder was successfully milled into the bimodal powder (at ~1.1 and ~2.2 μm). For the bimodal AlON powder, the gap filling ability of the small particles between large particles was found to be favorable for the fast densification process.[23,24]

B. Characteristics of processed AlON ceramics

After being processed by the SPS at 1350 °C, 1400 °C, 1450 °C, and 1500 °C for 10 min, respectively, high density γ-AlON ceramics were obtained. As shown in Table I, the density of the sintered sample is 3.69–3.74 g/cm^3. The measured temperatures shown in Fig. 4(a) reveal that the sintering temperature overshot the set temperature during heating. The corresponding overshoot temperature is 1425, 1458, 1477, and 1509 °C for the samples held at 1350, 1400, 1450, and 1500 °C. Assuming that the phase composition of the sintered sample is based on the γ-AlON single phase during heating, the densification kinetics curves have been calculated and are shown in Fig. 4(b). Figure 4(b) reveals that the main shrinkage of all the samples has occurred during the first ramping up period, and the relative density has already reached 98.72% when the respective specimen was heated up to 1425 °C. Therefore, the bimodal AlON powder can be fast densified during the fast heating (100 °C/min) of the SPS process, and the high density of the obtained samples should be mainly benefited from the higher first step sintering temperature.

The phase composition analysis of all the sintered samples is shown in Fig. 1. It reveals that besides the major γ-AlON phase, some minor amounts of α-Al_2O_3 and h-AlN phases could be also detected in the samples fabricated at 1350 and 1400 °C. It has been demonstrated that AlON particles are firstly transformed into Al_2O_3 and AlN at low temperatures which then form the AlON phase again at high temperatures.[22,25] Moreover, the phase

TABLE I. Density of the samples after holding 10 min at different temperatures.

Temperature (°C)	1350	1400	1450	1500
Density (g/cm^3)	3.70	3.74	3.69	3.69

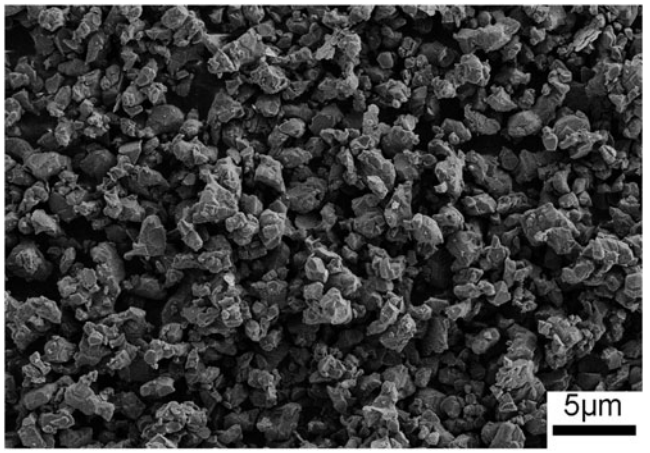

FIG. 3. SEM image of the milled AlON powder.

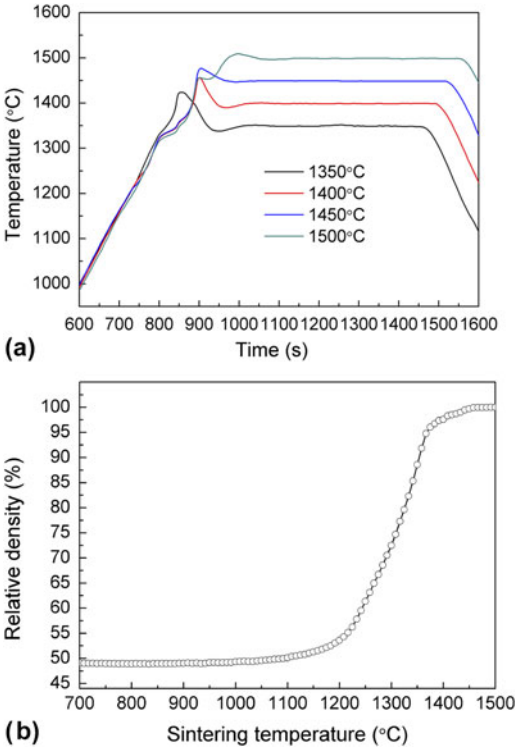

FIG. 4. Sintering temperature (a) and densification kinetics curves (b) of the bimodal AlON powder.

structure of Al_2O_3 depends on the particle size of AlON powder, namely, the fine AlON particles were transformed into hexagonal α-Al_2O_3 and h-AlN, while coarse AlON particles were transformed into cubic η-Al_2O_3 and h-AlN.[15,22] In the SPS-processed samples (held 10 min at 1350 and 1400 °C) prepared from the bimodal AlON powder, γ-AlON, α-Al_2O_3, and h-AlN were detected instead of the η-Al_2O_3, α-Al_2O_3, and h-AlN phases, which indicates that either the coarse particles keep their AlON phase due to the fast heating rate (100 °C/min) combined with the structural similarity between cubic γ-AlON and η-Al_2O_3 or the holding period (10 min) contributes to the retransformation from η-Al_2O_3 and AlN to γ-AlON. Therefore, in the SPS processing of the bimodal AlON powder, the AlON phase should be favored by the coarse γ-AlON particles, and the α-Al_2O_3 and h-AlN phases are formed from the fine γ-AlON particles in the powder. In addition, the XRD patterns shown in Fig. 1 also reveal that in the SPS process, α-Al_2O_3 and h-AlN retransform into γ-AlON after sintering temperature is increased, α-Al_2O_3 cannot be detected in the sample held at 1450 °C, and single phase γ-AlON ceramics were obtained when sintering temperature increased to 1500 °C. It is noted that the phase transformation temperature from Al_2O_3 and AlN to AlON is lower than that of the traditional pressureless sintering, 1450 °C versus 1700 °C.[22] It is noticeable that although a small amount of the h-AlN phase can be detected in samples sintered at 1450 °C, and the density of h-AlN is lower than cubic γ-AlON and α-Al_2O_3 (Table II), the SPS-processed sample shows the same density as that of the γ-AlON phase. It suggests that for the sample sintered at 1350–1450 °C, the effect of h-AlN on the density may be ignored, for only a small amount of the h-AlN phase can be detected in the three samples sintered at 1350 °C, 1400 °C, and 1450 °C (Fig. 1). As shown in Table II, the density of α-Al_2O_3 (3.99 g/cm^3) is higher than that of γ-AlON (3.69 g/cm^3), so not taking into account AlN, 8.2 wt% and 15.1 wt% Al_2O_3 are present in samples sintered at 1350 °C and 1400 °C, respectively, according to the XRD patterns shown in Fig. 1, which leads to the samples fabricated at 1350 °C and 1400 °C having a density of 3.71 g/cm^3 and 3.73 g/cm^3 based on the rule of mixture. It is noticed that the calculated density of 3.71 g/cm^3 and 3.73 g/cm^3 is close to the tested density values of 3.70 g/cm^3 and 3.74 g/cm^3 shown in Table I, respectively. Therefore, the higher density of 3.70 and 3.74 g/cm^3 (Table I) of samples sintered at 1350 and 1400 °C should be attributed to the formation of α-Al_2O_3. Moreover, due to the greater amount of α-Al_2O_3 (15.1 wt%) detected in samples sintered at 1400 °C than in those sintered at 1350 °C (8.2 wt%), the higher density was measured for the samples sintered at 1400 °C than for those sintered at 1350 °C. Therefore, the higher density of 3.70 and 3.74 g/cm^3 (Table I) of the samples sintered at 1350 and 1400 °C should be attributed to the formation of α-Al_2O_3. Moreover, due to the higher amount of the α-Al_2O_3 phase (15.1 wt%) detected in samples sintered at 1400 °C than that in the samples sintered at 1350 °C (8.2 wt%), the higher density of 3.74 g/cm^3 was measured for the sample sintered at 1400 °C than for the one sintered at 1350 °C.

TABLE II. Density of γ-AlON, α-Al_2O_3, and h-AlN.

Materials	γ-AlON	α-Al_2O_3	h-AlN
Density (g/cm^3)	3.69	3.99	3.25

Figure 5 shows all the transparent samples and their measured transmittance (1.2 mm in thickness) fabricated at 1350–1500 °C. Despite being three-phase materials, the obtained samples sintered at 1350 °C and 1400 °C exhibited high infrared transparency. The maximum infrared transmittance of SPS-processed samples at 1350 °C for 10 min is 77.3% at ~3900 nm, which is similar to that of the samples pressureless sintered at 1880 °C for 90 min.[15] These results indicate that the SPS sintering temperature can be decreased by about 500 °C and holding time can be shortened by 80 min when using SPS technique for the consolidation of the bimodal AlON powder. It is worth noticing that this is the first known work which succeeded in fabricating transparent AlON ceramics at such low temperatures by SPS technology. Moreover, for the present AlON sample with a thickness of 1.2 mm, its maximum infrared transmittance is slightly higher (2.1%) than that of the specimen with thickness of 0.5 mm, SPS-processed at 1700 °C by using Al_2O_3, and AlN as starting materials.[27] However, compared with the best obtained transmittance of the AlON specimens sintered by the conventional pressureless sintering method (1850 °C held for 6 h, 1 mm in thickness),[13] the transmittance of the SPS-processed AlON ceramics is slightly lower, 83.3% versus 77.3%. Optimization of the processing, based on the heating rate, holding time, pressure etc.,

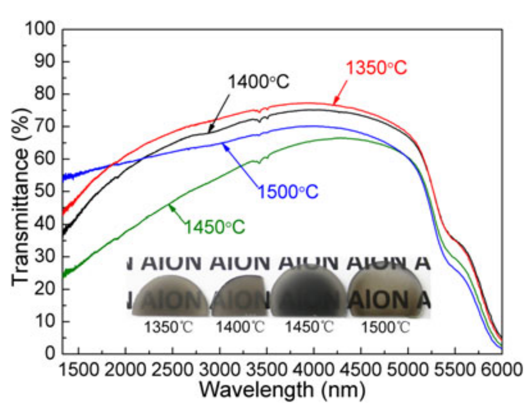

FIG. 5. Transparent samples and their transmittance curves.

should be able to further improve the transmittance of the SPS-processed AlON ceramics.

Additionally, as illustrated in Fig. 5, the transmittance of fabricated samples decreases when the sintering temperature increased from 1350 °C to 1450 °C at whole wavelength range of 1330–6000 nm. However, under further increased sintering temperature to 1500 °C, the transmittance of the obtained single phase AlON ceramics was obviously improved at near visible wavelength, i.e., from being at 25.0% for the sample held at 1450 °C the transmittance increased up to 54.7% for the sample obtained at 1500 °C.

As shown in Fig. 6, no visible pores can be observed at the fracture surfaces of all the sintered samples. Therefore, the high infrared transmittance of the obtained three-phase AlON ceramics should be mainly attributed to their high density [Figs. 6(a) and 6(b) and Table I]. Figs. 6(a) and 6(b) also reveal that the sample structure is predominantly represented by small size grains. Most grains are about 5–10 μm, but some very small grains of less than 2–3 μm can be observed too. Since α-Al_2O_3 and h-AlN phases are formed from fine AlON particles, the phase compositions of the smaller grains in the sintered samples should mainly be based on the α-Al_2O_3 and h-AlN phases. Therefore, the reason of why the produced three-phase material does not compromise infrared properties at longer wavelength of >3000 nm can be attributed to the grain size effect of small α-Al_2O_3 and h-AlN grains, which results in lower scattering at long wavelength band.[26] On the contrary, the small α-Al_2O_3 and h-AlN grains result in higher scattering in short wave length range, and the respective sample shows lower transmittance at the wavelength of <3000 nm (Fig. 5). In addition, the small refraction index difference of ~0.13[28,29] between major phase AlON and minor phase α-Al_2O_3 (the effect of h-AlN is negligible due to its lower content, as shown in Fig. 1) can be another reason to explain the high infrared transparency of the obtained samples. Therefore, after increasing the sintering temperature up to 1500 °C and thus enabling the α-Al_2O_3 and h-AlN phases' retransformation into the γ-AlON phase (Fig. 1), the obtained single phase AlON with >4–5 μm grains [Fig. 6(d)] shows an improved transmittance at near visible band, but its infrared transmittance is lower about 7% than that of the sample held at 1350 °C. Hence, the grain size should be the other importance reason to influence the transparency of AlON ceramics. Adjusting the initial particle size combined with SPS processing parameters controlled to improve the grain size distribution of AlON ceramics should be a promising approach to improve the transparency of the processed AlON ceramics. Additionally, the hardness measurements indicate that the fabricated AlON ceramics at 1350 °C has high hardness of 17.81 GPa, which is slightly higher (1.69 GPa) than that of the specimen fabricated by the conventional method (1860–1880 °C for 10 h).[11] The high hardness of the SPS sintered AlON should be attributed to its small grain size of <10 μm caused by the high heating rate, low sintering temperature, and short holding time. More processing approaches should be explored to control the single phase AlON grain sizes within a desired range.

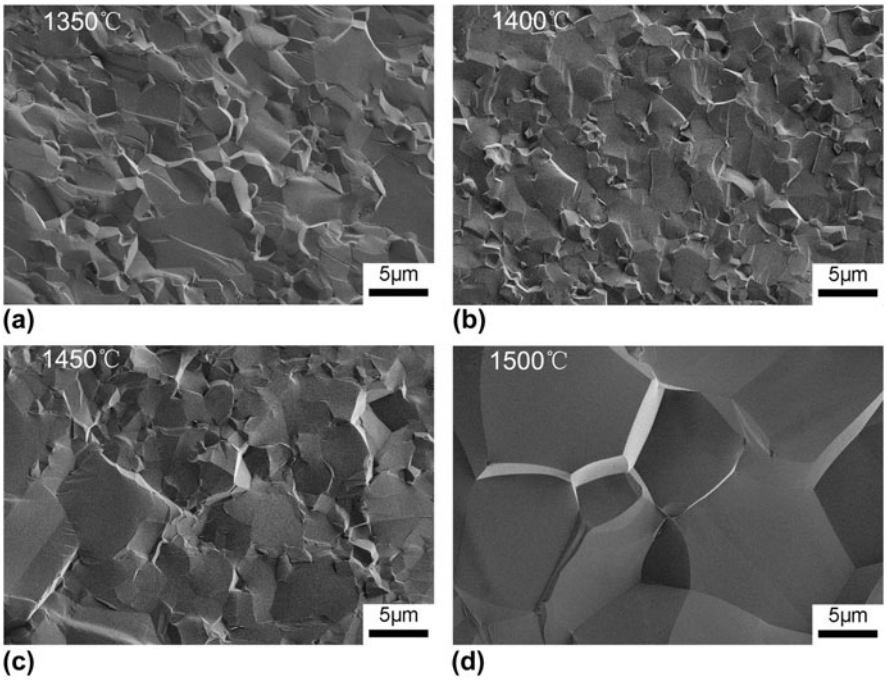

FIG. 6. SEM images of the fracture surfaces of the sintered AlON ceramics.

IV. CONCLUSION

The bimodal γ-AlON powder synthesized by the CRN method can be rapidly densified during fast heating (100 °C/min) of the SPS process, and high density γ-AlON ceramics were fabricated at 1350–1500 °C after holding 10 min. Moreover, highly infrared transparent AlON ceramics have been produced by the SPS of the bimodal γ-AlON powder at the low temperature of 1350 °C. Despite being three-phase (γ-AlON, α-Al_2O_3, and h-AlN) materials, the obtained samples showed high infrared transparency: the maximum transmittance in the medium infrared region could reach 77.3% at ~3900 nm for 1.2 mm thick specimens. At the same time, the sintered samples have high hardness of 17.81 GPa. The high infrared transparency of the obtained samples should be mainly attributed to their high density. Also, the smaller size of α-Al_2O_3 and h-AlN grains, as well as the small refraction index difference between AlON and α-Al_2O_3 phases, should further benefit the high infrared transmittance of the obtained ceramics. In addition, the high density and small grain size contribute also to the high hardness of the processed transparent ceramics.

ACKNOWLEDGMENT

The support of the US researchers by the US Department of Energy, Materials Sciences Division, under Award No. DE-SC0008581 is gratefully acknowledged. This work has been supported also by the Fundamental Research Funds for the Central Universities (3132015097, 3132016329), China Scholarship Council (201506575020).

REFERENCES

1. J.W. MaCauley, P. Patel, M. Chen, G. Gilde, E. Strassburger, B. Paliwal, K.T. Ramesh, and D.P. Dandekar: AlON: A brief history of its emergence and evolution. *J. Eur. Ceram. Soc.* **29**, 223–226 (2009).
2. M.Y. Su, Y.F. Zhou, K. Wang, Z.F. Yang, Y.G. Cao, and M.C. Hong: Highly transparent AlON sintered from powder synthesized by direct nitridation. *J. Eur. Ceram. Soc.* **35**, 1173–1178 (2015).
3. R.J. Xie, N. Hirosaki, X.J. Liu, T. Takeda, and H.L. Li: Crystal structure and photoluminescence of Mn^{2+}–Mg^{2+} codoped gamma aluminum oxynitride (γ-AlON): A promising green phosphor for white light-emitting diodes. *Appl. Phys. Lett.* **92**, 201905 (2008).
4. J.J. Swab, R. Pavlacka, G. Gilde, S. Kilczewski, J. Wright, and D. Harris: Determining the strength of coarse-grained AlON and spinel. *J. Am. Ceram. Soc.* **97**, 592–600 (2013).
5. B.T. Tu, H. Wang, X. Liu, W.M. Wang, and Z.Y. Fu: First-principles study on site preference of aluminum vacancy and nitrogen atoms in γ-AlON. *J. Am. Ceram. Soc.* **96**, 1937–1943 (2013).
6. X.L. Li, J.M. Luo, and Y. Zhou: Spark plasma sintering behavior of AlON ceramics doped with different concentrations of Y_2O_3. *J. Eur. Ceram. Soc.* **35**, 2027–2032 (2015).
7. F. Zhang, S.W. Wang, X.J. Liu, L.Q. An, and X.Y. Yuan: Upconversion luminescence in Er-doped gamma-AlON ceramic phosphors. *J. Appl. Phys.* **105**, 093542 (2009).
8. F. Zhang, S. Chen, J.F. Chen, H.L. Zhang, J. Li, X.J. Liu, and S.W. Wang: Characterization and luminescence properties of AlON:Eu^{2+} phosphor for white-emitting-diode illumination. *J. Appl. Phys.* **111**, 083532 (2012).
9. X.D. Wang, F.M. Wang, and W.C. Li: Synthesis, microstructures and properties of γ-aluminum oxynitride. *Mater. Sci. Eng., A* **342**, 245–250 (2003).
10. F. Chen, F. Zhang, J. Wang, H.L. Zhang, R. Tian, J. Zhang, Z. Zhang, F. Sun, and S.W. Wang: Microstructure and optical properties of transparent aluminum oxynitride ceramics by hot isostatic pressing. *Scr. Mater.* **81**, 20–23 (2014).
11. Y. Wang, X.M. Xie, J.Q. Qi, J. Wang, N. Wei, and T.C. Lu: Two-step preparation of AlON transparent ceramics with powder synthesized by aluminothermic reduction and nitridation method. *J. Mater. Res.* **29**, 2325–2331 (2014).
12. R.S. Kumar and R. Johnson: Aqueous slip casting of transparent aluminum oxynitride. *J. Am. Ceram. Soc.* **99**, 3220–3225 (2016).
13. Q. Liu, N. Jiang, J. Li, K. Sun, Y.B. Pan, and J.K. Guo: Highly transparent AlON ceramics sintered from powder synthesized by carbothermal reduction nitridation. *Ceram. Int.* **42**, 8290–8295 (2016).
14. A. Krell and A. Bales: Grain size-dependent hardness of transparent magnesium aluminate spinel. *Int. J. Appl. Ceram. Technol.* **8**, 1108–1114 (2011).
15. Y.C. Shan, J.X. Xu, G. Wang, X.N. Sun, G.H. Liu, J.J. Xu, and J.T. Li: A fast pressureless sintering method for transparent AlON ceramics by using a bimodal particle size distribution powder. *Ceram. Int.* **41**, 3992–3998 (2015).
16. E. Khaleghi, Y.S. Lin, M.A. Meyers, and E.A. Olevsky: Spark plasma sintering of tantalum carbide. *Scr. Mater.* **63**, 577–580 (2010).
17. E.A. Olevsky, W.L. Bradbury, C.D. Haines, D.G. Martin, and D. Kapoor: Fundamental aspects of spark plasma sintering: I. Experimental analysis of scalability. *J. Am. Ceram. Soc.* **95**, 2406–2413 (2012).
18. R. Orru, R. Licheri, A.M. Locci, A. Cincotti, and G. Cao: Consolidation/synthesis of materials by electric current activated/assisted sintering. *Mater. Sci. Eng., R* **63**, 127–287 (2009).
19. G.D. Cui, X.L. Wei, E.A. Olevsky, R.M. German, and J.Y. Chen: Preparation of high performance bulk Fe–N alloy by spark plasma sintering. *Mater. Des.* **90**, 115–123 (2016).
20. K. Hu, X.Q. Li, S.G. Qu, and Y.Y. Li: Effect of heating rate on densification and grain growth during spark plasma sintering of 93W–5.6Ni–1.4Fe heavy alloys. *Metall. Mater. Trans. A* **44**, 4323–4336 (2013).
21. I.W. Chen and X.H. Wang: Sintering dense nano-crystalline ceramics without final stage grain growth. *Nature* **404**, 168–171 (2000).
22. Y.C. Shan, Z.H. Zhang, X.N. Sun, J.J. Xu, Q.H. Qin, and J.T. Li: Fast densification mechanism of bimodal powder during pressureless sintering of transparent AlON ceramics. *J. Eur. Ceram. Soc.* **36**, 671–678 (2016).
23. A. Wonisch, T. Kraft, M. Moseler, and H. Riedel: Effect of different article size distributions on solid-state sintering: A microscopic simulation approach. *J. Am. Ceram. Soc.* **92**, 1428–1434 (2009).
24. A. Petersson and J. Ågren: Sintering shrinkage of WC-Co materials with bimodal grain size distributions. *Acta Mater.* **53**, 1665–1671 (2005).
25. H.X. Willems, M.M.R.M. Hendrix, G. de With, and R. Metselaar: Thermodynamics of AlON. II. Phase relations. *J. Eur. Ceram. Soc.* **10**, 339–346 (1992).
26. M.I. Jones, H. Hyuga, and K. Hirao: Optical and mechanical properties of α/β composite sialons. *J. Am. Ceram. Soc.* **86**, 520–522 (2003).

27. W. Wei, Z.Y. Fu, H. Wang, and W.M. Wang: Research on AlON transparent ceramics by SPS. *J. Wuhan Univ. Technol.* **31**, 13–14, 44 (2009).
28. J. Kischkat, S. Peters, B. Gruska, M. Semtsiv, M. Chashnikova, M. Klinkmüller, O. Fedosenko, S. Machulik, A. Aleksandrova, G. Monastyrskyi, Y. Flores, and W.T. Masselink: Mid-infrared optical properties of thin films of aluminum oxide, titanium dioxide, silicon dioxide, aluminum nitride, and silicon nitride. *Appl. Opt.* **51**, 6789–6798 (2012).
29. T.M. Hartnett, S.D. Bernstein, E.A. Maguire, and R.W. Tustison: Optical properties of AlON (aluminum oxynitride). *Infrared Phys. Technol.* **39**, 203–211 (1998).